

MODELING AND SIMULATION OF NO_x/SO₂ REMOVAL IN AN AQUEOUS
SCRUBBER SYSTEM USING THE ADDITIVE Fe(II)*EDTA

by

RECEIVED

FEB 16 1995

OSTI

Wen Li, M. Mendelsohn, J.B.L. Harkness, and C.D. Livengood

Argonne National Laboratory
9700 South Cass Avenue
Argonne, Illinois 60439

Satish Parulekar

Chemical Engineering Department
Illinois Institute of Technology
Chicago, Illinois 60616

Prepared for Publication in

Environmental Progress

Sponsored by

American Institute of Chemical Engineering

DISTRIBUTION OF THIS DOCUMENT IS UNLIMITED 85

The submitted manuscript has been authored
by a contractor of the U. S. Government
under contract No. W-31-109-ENG-38.
Accordingly, the U. S. Government retains a
nonexclusive, royalty-free license to publish
or reproduce the published form of this
contribution, or allow others to do so, for
U. S. Government purposes.

DISCLAIMER

This report was prepared as an account of work sponsored by an agency of the United States Government. Neither the United States Government nor any agency thereof, nor any of their employees, makes any warranty, express or implied, or assumes any legal liability or responsibility for the accuracy, completeness, or usefulness of any information, apparatus, product, or process disclosed, or represents that its use would not infringe privately owned rights. Reference herein to any specific commercial product, process, or service by trade name, trademark, manufacturer, or otherwise does not necessarily constitute or imply its endorsement, recommendation, or favoring by the United States Government or any agency thereof. The views and opinions of authors expressed herein do not necessarily state or reflect those of the United States Government or any agency thereof.

MASTER

DISCLAIMER

Portions of this document may be illegible in electronic image products. Images are produced from the best available original document.

MODELING AND SIMULATION OF NO_x/SO₂ REMOVAL IN AN AQUEOUS SCRUBBER SYSTEM USING THE ADDITIVE Fe(II)*EDTA¹

Wen Li, M. Mendelsohn, J.B.L. Harkness, and C.D. Livengood
Argonne National Laboratory
9700 South Cass Avenue
Argonne, Illinois 60439

Satish Parulekar
Chemical Engineering Department
Illinois Institute of Technology
Chicago, Illinois 60616

ABSTRACT

Addition of the metal chelate, ferrous*ethylenediaminetetraacetate anion (Fe(II)*EDTA²⁻), has been shown to increase the amount of gaseous nitrogen oxides (NO_x) absorbed from a gas stream containing sulfur dioxide (SO₂), where an aqueous scrubbing process is used to treat the gas. Recently, we published and presented data on improved systems for NO_x removal that incorporate an antioxidant and/or reducing agent (A/R) in the process, together with the Fe(II)*EDTA. In this paper, a mathematical model describing NO_x removal as a function of the square root of Fe(II)*EDTA concentration in the solution and of the operating conditions is derived and validated.

¹ Work supported by the U.S. Department of Energy, Assistant Secretary for Fossil Energy, under contract W-31-109-Eng-38.

1 Introduction

Previous investigations have shown that addition of the metal chelate, ferrous*ethylenediaminetetraacetate anion (Fe(II)*EDTA^{2-}), can increase the amount of gaseous nitrogen oxides (NO_x) absorbed from a gas stream containing sulfur dioxide (SO_2), where an aqueous scrubbing process is used to treat the gas.^{1,2,3} Compared with some other metal chelates, ferrous*EDTA has the advantages of moderate cost, reasonable stability, high solubility, lack of gummy residues, excellent equilibrium constant for forming a complex with NO, and rapid kinetics for absorption of NO. One disadvantage of ferrous*EDTA is that it is readily oxidized to Fe(III)*EDTA , a much less efficient absorbent for NO.

In previous work, we have presented data on a laboratory scrubber system for NO_x removal that incorporates an antioxidant and/or reducing agent (A/R) in the process, together with Fe(II)*EDTA .^{4,5} The purpose of the A/R is to maintain the highest possible concentration of iron in the +2 form.

Three important variables for iron EDTA processes are the scrubber size, the liquid-to-gas ratio of the scrubber, and the fraction of Fe(II)*EDTA oxidized. These variables have important impacts, either on the NO_x removal or on the annual cost requirements of a process. Hence, a method of predicting scrubber performance is needed if the full-scale annual revenue requirements of a process utilizing Fe(II)*EDTA are to be estimated accurately when the system is scaled up.

In this paper, a mathematical model is derived that describes the dependence of NO_x removals on flue-gas flow rate and liquor flow rate in the absorber, Fe(II)*EDTA

concentration, absorber length, and gas-liquid interfacial area. The model can also lead to insights on (1) the importance of the various mechanisms affecting NO removal and (2) the differences in NO_x-removal behaviors observed with different chemistries.

2 Derivation of Model Equation for NO_x Removal

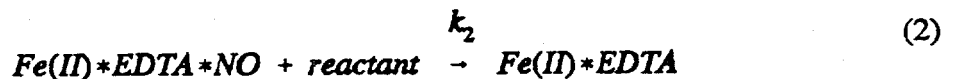
A substantial number of reactions are responsible for the removal of NO by using Fe(II)*EDTA. These reactions can be grouped into four major types: complexation, regeneration, oxidation, and reduction.

In the complexation reaction, NO is complexed with ferrous*EDTA to form a nitrosyl oxide complex. The reaction can be described as:

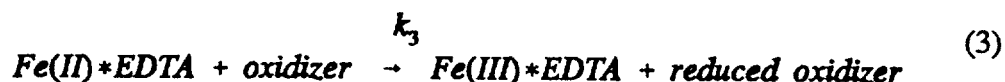


The regeneration reaction involves reaction of nitrosyl oxide complex with such species as sulfite and bisulfite, to free the Fe(II)*EDTA for further NO absorption.

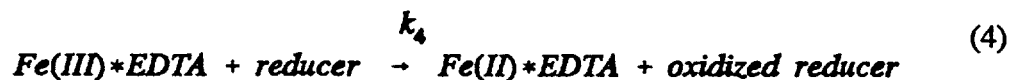
The reaction can be described as:



Fe(II)*EDTA is oxidized to Fe(III)*EDTA in the presence of an oxidizer (such as oxygen) in the flue gas. Such oxidation causes NO removal to decline. The general oxidation reaction is



Fe(II)*EDTA can be generated from Fe(III)*EDTA by addition of additives, such as ascorbate, via the following typical reduction reaction:



In the experimental studies, our focus is on removal of NO from the gas phase. So far as NO removal is concerned, although all the reactions described above are important, the key reaction is the formation of a complex between NO and Fe(II)*EDTA. In a mathematical model of such a reaction scheme, the larger the number of reactions considered, the larger the number of kinetic parameters (Arrhenius exponential coefficient, activation energy, and reaction orders) that need to be estimated, and therefore the greater the number of species in the reaction phase (liquid phase) that must be monitored.

The experimental data available contain information only on NO and total

Fe(II)*EDTA (with/without complexing with NO). In the design of large-scale absorbers, one is normally most interested in the rate of NO removal from the gas phase (absorption of NO from the gas phase, followed by reaction of NO with Fe(II)*EDTA in the liquid phase to form Fe(II)*EDTA*NO). With respect to NO removal, one is less concerned about what happens to the Fe(II)*EDTA*NO (i.e., regeneration of Fe(II)*EDTA via formation of N-S compounds, etc.). Owing to lack of information on concentrations of such species as Fe(II)*EDTA*NO, Fe(III)*EDTA, N-S complex, and ascorbate and its de-oxy form in the absorber, we consider reactions involving these species to be faster than the reaction between Fe(II)*EDTA and NO. The rate of removal of NO from the gas phase is controlled by the rate of this reaction. Therefore, in the mathematical model presented here, we only consider the reaction



and consider NO to be the dominant component of NO_x in flue gases, which indeed was the case for the experiments discussed here. At least 95% of the total measured NO_x in our synthetic flue gas consisted of NO. Other oxides of nitrogen, such as NO₂, were present in trace amounts.

The rate of reaction 5 is assumed to be first-order in NO and first-order in Fe(II)*EDTA, as found by several previous investigators.^{6,7,8} The rate of this reaction can be represented as:

$$r_{NO} = K C_{Fe(II)L} C_{NO} \quad (6)$$

where:

K = Reaction rate constant, L/mole•hr

r_{NO} = Rate of removal of NO, mole/L•hr

$C_{Fe(II)L}$ = Concentration of Fe(II)*EDTA, mole/L

C_{NO} = Concentration of NO in liquid phase, mole/L

To describe NO removal from the gas phase (by conversion into the liquid phase) and subsequent consumption of NO by chemical reaction, we must consider mass transfer and reaction processes in the boundary layer (film) near the gas-liquid interface in the liquid phase and in the bulk liquid phase, as well as the gas-phase mass-transfer process in the film near the gas-liquid interface (Figure 1). Since the velocity of the gas phase in the reactor is much greater than the velocity of the liquid phase, the thickness of the gas-side boundary layer and concentration gradients across the gas-side boundary layer are negligible.

[INSERT FIGURE 1 HERE]

In our model, we consider that reaction 5 mostly occurs in the liquid film (i.e., concentration of NO in the bulk liquid is negligible compared with that at the gas-liquid interface). The extent of reaction 5 in the bulk liquid is therefore considered to be negligible. Other reactions may occur largely in bulk liquid or liquid film or anywhere in the liquid phase; because these reactions do not involve NO as a reactant

or a product, we do not place any restrictions on where they occur. We focus only on the liquid-side film (boundary layer) where diffusion and chemical reaction occur simultaneously. The mass balances for NO and Fe(II)*EDTA in the liquid-side film (δ_L) are:

$$D_{NO} \frac{d^2 C_{NO}}{dx^2} - r_{NO} = 0, \quad 0 < x < \delta_L \quad (7)$$

and

$$D_{Fe^{2+}} \frac{d^2 C_{Fe(II)L}}{dx^2} - r_{NO} = 0, \quad 0 < x < \delta_L \quad (8)$$

In the mass balance equations above, we consider variations in concentration/partial pressure only, because in the two-phase (gas-liquid) reactor, the volumetric flow rate of the gas phase is much greater than that of the liquid phase. The gas phase (in the form of bubbles) usually moves in the form of plug flow. In plug flow, concentration and velocity gradients in directions perpendicular to the axial direction are negligible.

Further, owing to the low solubility of NO in water, $C_{Fe(II)L} \gg C_{NO}$, depletion of Fe(II)*EDTA due to chemical reaction will be less significant (on a percent basis) than that of NO. Therefore, from the mass balance for Fe(II)*EDTA,

$$\frac{d^2 C_{Fe(II)L}}{dx^2} = 0, \quad 0 < x < \delta_L \quad (9)$$

or $C_{Fe(II)L} = ax + b$, where a, b are constants. Since Fe(II)*EDTA is nonvolatile,

$dC_{Fe(II)L}/dx = 0$ at $x = 0$ (gas-liquid interface), which implies that $a = 0$ and $C_{Fe(II)L} = b$

$= (C_{\text{Fe(III)}})_{\text{bulk liquid}}$. The reaction can therefore be considered to be pseudo-first-order in NO, since the extent of backmixing in the liquid phase greatly exceeds that in the gas phase. The axial variations in $C_{\text{Fe(III)}}$ are considered to be insignificant. The mass balance for NO in the liquid film now becomes:

$$D_{\text{NO}} \frac{d^2 C_{\text{NO}}}{dx^2} - K C_{\text{Fe(III)}} C_{\text{NO}} = 0, \quad 0 < x < \delta_L \quad (10)$$

$$C_{\text{NO}}(x=0) = C_{\text{NO}}^i = \frac{p_{\text{NO}}}{H}, \quad C_{\text{NO}}(x = \delta) \rightarrow 0 \quad (11)$$

where H is the Henry's law constant for NO. We consider the reaction to be sufficiently fast that it is largely completed in the liquid film. If p_{NO} is the partial pressure of NO in the bulk gas phase and $y = x/\delta_L$, then

$$\frac{D_{\text{NO}}}{\delta_L^2} \frac{d^2 C_{\text{NO}}}{dy^2} - K C_{\text{Fe(III)}} C_{\text{NO}} = 0, \quad 0 < y < 1, \quad (12)$$

i.e.,

$$\frac{d^2 C_{\text{NO}}}{dy^2} - \frac{K \delta_L^2 C_{\text{Fe(III)}}}{D_{\text{NO}}} C_{\text{NO}} = 0, \quad 0 < y < 1 \quad (13)$$

Let

$$\gamma^2 = \frac{K \delta_L^2 C_{\text{Fe(III)}}}{D_{\text{NO}}} \quad (14)$$

$$\frac{d^2 C_{NO}}{dy^2} - \gamma^2 C_{NO} = 0 \quad (15)$$

and

$$C_{NO} = A \cosh(\gamma y) + B \sinh(\gamma y) \quad (16)$$

At $y = 0$ ($x = 0$), $C_{NO} = C_{NO}^i = p_{NO}/H$ (i.e., $p_{NO}/H = A$) and at $y = 1$ ($x = \delta_L$),

C_{NO} goes to zero (concentration of NO in the bulk liquid is negligible in comparison to C_{NO}^i).

$$0 = \frac{p_{NO}}{H} \cosh(\gamma) + B \sinh(\gamma) \quad , \quad (17)$$

$$B = -\frac{p_{NO}}{H \tanh(\gamma)} \quad (18)$$

Thus,

$$C_{NO} = \frac{p_{NO}}{H} \left(\cosh(\gamma y) - \frac{\sinh(\gamma y)}{\tanh(\gamma)} \right) \quad (19)$$

The flux of absorption of NO at the gas-liquid interface is then obtained as:

$$N_{NO} = -D_{NO} \frac{dC_{NO}}{dx} \Big|_{x=0} = -\frac{D_{NO}}{\delta_L} \frac{dC_{NO}}{dy} \Big|_{y=0} \quad (20)$$

$$\frac{dC_{NO}}{dy} = \frac{p_{NO}}{H} \left(\gamma \sinh(\gamma y) - \frac{\gamma \cosh(\gamma y)}{\tanh(\gamma)} \right) \quad (21)$$

Thus,

$$N_{NO} = -\frac{D_{NO}}{\delta_L} \frac{P_{NO}}{H} \left(-\frac{\gamma}{\tanh(\gamma)} \right) \quad (22)$$

i.e.,

$$N_{NO} = \frac{D_{NO}}{\delta_L H} P_{NO} \left(\frac{\gamma}{\tanh(\gamma)} \right) \quad (23)$$

Next, we consider the mass balance for NO in the gas phase (Figure 2):

$$Q_g C_{NO}^g|_z - Q_g C_{NO}^g|_{z+dZ} - N_{NO} a \epsilon_L dZ A = \frac{\partial}{\partial t} (C_{NO}^g A dZ \epsilon_g) \quad (24)$$

where ϵ_L , ϵ_g = holdups of (volume fractions occupied by) liquid and gas phases, respectively.

A = Area of cross-section of empty reactor,

a = Gas-liquid interfacial area per unit liquid-phase volume (depends on diameter of gas bubbles), and

C_{NO}^g is related to partial pressure of NO in gas phase, p_{NO} , as follows:

$$C_{NO}^g = p_{NO}/RT$$

[INSERT FIGURE 2 HERE]

Since the "space time" for the gas phase (time spent by the gas in the reactor) is much less than that for the liquid phase, we can apply pseudo-steady-state considerations for the gas phase. The mass balance for NO in the bulk gas phase then assumes the form

$$-\frac{[Q_g p_{NO}|_{z+dz} - Q_g p_{NO}|_z]}{dz} - N_{NO} a \epsilon_L ART = 0 \quad (25)$$

i.e.,

$$\frac{d}{dz}(Q_g p_{NO}) = -N_{NO} a \epsilon_L ART \quad (26)$$

Since NO is usually dilute in the flue-gas stream, axial variation of Q_g can be neglected; then (in view of Eq. 23),

$$\frac{dp_{NO}}{dz} = -\frac{N_{NO} a \epsilon_L ART}{Q_g} = -\frac{D_{NO}}{\delta_L H} p_{NO} \frac{\gamma}{\tanh(\gamma)} \frac{a \epsilon_L ART}{Q_g} \quad (27)$$

i.e.,

$$\frac{dp_{NO}}{p_{NO}} = -\frac{D_{NO}}{\delta_L H} \frac{\gamma}{\tanh(\gamma)} \frac{a \epsilon_L ART}{Q_g} dz \quad (28)$$

Integrating the above gas-phase mass balance over the reactor (from bottom to top), we obtain

$$\ln \left(\frac{P_{NO,e}}{P_{NO,f}} \right) = - \frac{D_{NO}}{\delta_L H} \frac{a \epsilon_L RTV}{Q_g} \frac{\gamma}{\tanh(\gamma)} \quad (29)$$

When the reaction is fast, as the one under consideration is, $\tanh(\gamma) \rightarrow 1$. Partial pressures of NO in the gas feed and the gas effluent are denoted by $P_{NO,f}$ and $P_{NO,e}$ respectively. Percent removal of NO is defined as

$$\% \text{ Removal} = 100 \left(1 - \frac{P_{NO,e}}{P_{NO,f}} \right) \quad (30)$$

$$\frac{P_{NO,e}}{P_{NO,f}} = 1 - \frac{\% \text{ removal}}{100} \quad (31)$$

Thus,

$$\ln \left(\frac{P_{NO,e}}{P_{NO,f}} \right) = \ln \left(1 - \frac{\% \text{ rem.}}{100} \right) = - \frac{D_{NO}}{\delta_L H} \frac{a \epsilon_L RTV}{Q_g} \gamma \quad (32)$$

i.e.,

$$1 - \frac{\% \text{ rem}}{100} = \exp \left(- \frac{D_{NO} \gamma}{\delta_L H} \frac{a \epsilon_L RTV}{Q_g} \right) \quad (33)$$

$$\% \text{ rem} = 100 \left(1 - \exp \left(- \frac{D_{NO} a}{\delta_L} \frac{V}{Q_g} \frac{RT}{H} \epsilon_L \gamma \right) \right) \quad (34)$$

where V = volume of empty reactor, Q_g = volumetric flow rate of gas.

$$-\ln \left(1 - \frac{\% \text{ rem}}{100} \right) = \frac{D_{NO} a}{\delta_L} \frac{V}{Q_g} \frac{RT}{H} \epsilon_L \gamma \quad (35)$$

Since $\gamma = (k\delta_L^2 C_{Fe(II)}/D_{NO})^{1/2}$ is proportional to $C_{Fe(II)}^{1/2}$, a plot of $[-\ln(1 - \%rem/100)]$ vs. $C_{Fe(II)}^{1/2}$ should yield a straight line if the model discussed above is valid. $C_{Fe(II)}$ (concentration of Fe(II)*EDTA available for complex formation) is a fraction of total ferrous concentration ($C_{Fe(II)Total}$).

From the solution of the gas-phase mass balance for NO,

$$\begin{aligned}
 NTU = -\ln\left[1 - \frac{\%rem}{100}\right] &= \frac{D_{NO} a \epsilon_L}{\delta_L} \frac{L}{u_G} \frac{RT}{H} \frac{\sqrt{K} \delta_L}{\sqrt{D_{NO}}} \sqrt{C_{Fe(II)L}} \\
 &= \sqrt{D_{NO} K} a \epsilon_L \frac{L}{u_G} \frac{RT}{H} \sqrt{\frac{C_{Fe(II)L}}{C_{Fe(II)Total}}} \sqrt{C_{Fe(II)Total}}
 \end{aligned} \tag{36}$$

where:

NTU = NO_x removal efficiency expressed as number of transfer units,
dimensionless.

D_{NO} = Diffusivity of dissolved NO in absorber liquid = 4.1×10^{-5} cm²/sec @
50°C.

K = Reaction rate constant for reaction between NO and
Fe(II)*EDTA.

$C_{Fe(II)L}$ = Ferrous EDTA concentration in absorber liquid.

$C_{Fe(II)Total}$ = Total concentration of ferrous EDTA (ferrous*EDTA plus
ferrous*EDTA*NO).

$a\epsilon_L$ = Gas-liquid interfacial area per volume of contact zone.

L = Length of gas-liquid contact zone.

u_G = Superficial flue-gas velocity in absorber.

H = Henry's law constant for NO in water = 710.7 atm/M @ 50°C.

R = Universal gas constant.

T = Temperature of scrubber liquor, °C.

Since the experimental measurements refer to total Fe(II) concentration (concentration of Fe(II)*EDTA plus concentration of Fe(II)*EDTA*NO), at a given temperature, the plot of $-\ln[1 - \%rem/100]$ vs. $C_{Fe(II)Total}^{1/2}$, if linear, would provide information on the fraction of Fe(II)*EDTA fed initially to the reactor that is available for reaction with NO. This fraction is expected to vary with the different scrubber chemistries. The slope of a plot is given by:

$$-\ln\left[1 - \frac{\%rem.}{100}\right] \quad \text{vs.} \quad \sqrt{C_{Fe(II)Total}} = \text{Slope} \quad (37)$$

$$\text{Slope} = \sqrt{D_{NO}} a \epsilon_L \frac{RT}{H} \frac{L}{u_G} \sqrt{K \frac{C_{Fe(II)L}}{C_{Fe(II)Total}}} \quad (38)$$

Figure 3 shows the NO_x removal (as number of transfer units, NTU) as a function of C_{FeTotal} with Fe(II)*EDTA and ascorbate addition in the different FGD chemistries. As can be seen from the figure, a very good linear fit is obtained between these two variables, demonstrating that the model we derived above is valid for the process. The slopes indicated in the figure decrease in the following order: sodium carbonate > magnesium-enhanced lime > hydrated lime. If the scrubber is operated under the nearly identical conditions in these chemistries, that means the parameters a, L, u_G, T in Eq. 35 are the same and, since the temperature is the same,

the reaction rate constant K is also the same. The ratio of $C_{\text{Fe(II)L}}/C_{\text{Fe(II)Total}}$ can be calculated using Eq. 38, sodium carbonate : magnesium-enhanced lime : hydrated lime = 2.2 : 1.5 : 1. It was found that the larger the ratio obtained, the higher was the concentration of Fe(II)*EDTA in the scrubber solution; therefore, higher NO removal was achieved. The reason the ferrous concentrations differ in the different chemistries will be discussed in the following section.

[INSERT FIGURE 3 HERE]

3 Discussion of the Model

Effect of Gas Bubble Size on the Model

The gas-liquid interfacial area (a) depends on the diameter of gas bubbles (d_B), which in turn depends on such parameters as sparger characteristics, physical properties of gas and liquid phases, and interfacial tension between gas and liquid phases. The size of individual bubbles can vary during their vertical passage in the reactor due to a variety of effects. Usually, in the design of gas-liquid reactors, one considers an average gas-bubble diameter, regarded as uniform throughout the reactor. The smaller the bubble size, the greater is the gas-liquid interfacial area.

It is very difficult to predict the effect of solids formation (products) on the size of gas bubbles in the scrubber system. During their passage through the scrubber, individual gas bubbles are subject to breakage, coalescence, drainage of liquid film surrounding bubbles, and collision with reactor walls and/or any solids in the reactor; each of these effects can change the size of bubbles. In continuous operation of

scrubbers, solids accumulation is inevitable. The size of gas bubbles in the bottom portion of the scrubber (near the gas sparger) is controlled by sparger characteristics and will not be affected by accumulation of solids. If the solids are well dispersed in the liquid, then solid particles will move along with the liquid phase in the scrubber. In this situation, the bubble size will be affected by all of the factors mentioned above, and determination of the exact effect of solids on changes in bubble size will be very difficult. More frequently, the solids will tend to accumulate near the bottom of the scrubber. In such a situation, to ensure effective functioning of the sparger without any blockage by solid products, one must make sure that solids do not accumulate above the sparger location.

Effect of Sulfite/Bisulfite on NO Removal

As mentioned above, NO removal is partly dependent on the concentration of Fe(II)*EDTA in the scrubber solution. The ratio of Fe(II)*EDTA concentration to total ferrous concentration in scrubber solution was found to vary with different FGD chemistries. A plausible explanation for this effect is the much-reduced solubility of sulfite ions in a lime environment compared with a sodium environment. In fact, sodium sulfite is about 10,000 times more soluble than calcium sulfite. The role of sulfite ions in the overall process concept is summarized in Figure 4. As the schematic shows, sulfite obtained via SO₂ dissolution from the flue gas plays an integral role in at least four important mechanisms in the simultaneous NO_x/SO₂ removal process and may in fact be the crucial factor in determining the success or failure of the process.

[INSERT FIGURE 4 HERE]

First, sulfite plays a critical role in NO removal performance by decomposing the complex Fe(II)*EDTA*NO in order to release more Fe(II)*EDTA for further absorption of NO and/or to release Fe(III)*EDTA for reduction to Fe(II)*EDTA . This mechanism has been reviewed in detail in Section 2.

Second, sulfite/bisulfite ions should play a critical role in the reduction of oxidized ascorbate (DHA) back to ascorbate. This is indicated by the work discussed in Section 4, which shows that the overall reaction rate for reduction of DHA by sulfite is directly proportional to the total sulfite/bisulfite concentration.

Third, sulfite ion itself also can reduce Fe(III)*EDTA back to Fe(II)*EDTA by means of natural reduction, which has been described and tested in previous work. Since this kind of reduction reaction rate is too slow to be practical, additional measures have to be taken to enhance the reaction rate, such as elevating the temperature.

Finally, sulfite ion reacts with hydrated lime to form a calcium sulfate slurry, which is the primary mechanism of removing SO_2 from the flue gas by FGD wet scrubber.

Overall, the sulfite plays important roles in maintaining a high ferrous concentration in the scrubber solutions, which in turn determines the NO removal. This explains why sodium carbonate chemistry achieved the highest NO removal, while hydrated lime provided poor NO removal.

What is necessary, then, in a practical system is to have sufficient sulfite and ascorbate concentrations so that the overall oxidation rate of Fe(II)*EDTA is balanced by the overall reduction rate of Fe(III)*EDTA, which can be used to maintain a constant Fe(II)*EDTA concentration in a pseudocatalytic process without the addition of other chemicals (that is, besides sulfite from absorption of gaseous sulfur dioxide). Bench experiments were performed to determine these concentrations by measuring ferrous concentrations in a solution containing sodium ascorbate and sodium sulfite, and through which air was bubbled. At various times, samples were withdrawn and the ferrous concentration in the sample was measured spectrophotometrically using 1,10 phenanthroline. The results of four different tests are shown in Figure 5. The figure shows that with a sulfite to iron ratio of 3:1, the ferrous concentration was maintained at a constant level for about 2 hours. Without continuous addition of sulfite, the ferrous concentration would not be expected to remain constant indefinitely. However, it would be very difficult to prove this concept in the current configuration of the laboratory-scale scrubber system because longer-duration tests are required, which will cause too much solid to form for continuous operation. The longer-term experiments are still being planned.

[INSERT FIGURE 5 HERE]

5 References

1. Harkness, J.B.L, and R.D. Doctor, *Development of Combined Nitrogen Oxide/Sulfur Oxide Environmental-Control Technology*, Argonne National Laboratory Report ANL/ECT-14 (Aug. 1985).
2. Harriott, P., K. Smith, and L.B. Benson, "Simultaneous Removal of NO and SO₂ in Packed Scrubbers or Spray Towers," *Environmental Progress*, Vol. 12, No. 2, p. 110, 1993.
3. Mendelsohn, M.H., C.D. Livengood, and J.B.L. Harkness, "Combined SO₂/NO_x Control Using Ferrous*EDTA and a Secondary Additive in a Lime-Based Aqueous Scrubber System," 1991 SO₂ Control Symposium, Vol. 2, Session 5B - Paper 7, Washington, D.C. (Dec. 3-6, 1991).
4. Mendelsohn, M.H., and J.B.L. Harkness, "Enhanced Flue-Gas Denitrification Using Ferrous*EDTA and a Polyphenolic Compound in an Aqueous Scrubber System," *Energy Fuels* 5: 244-48 (1991).
5. Mendelsohn, M.H., C.D. Livengood, and J.B.L. Harkness, "Further Studies of NO_x Control in Aqueous Scrubbers Using Ferrous*EDTA," Seventh Annual Coal Preparation, Utilization, and Environmental Control Contractor's Conference, Pittsburgh, Penn. (July 1991).

6. Littlejohn, D., and S.G. Chang, "Kinetic Study of Ferrous Nitrosyl Complexes," American Chemical Society, 86(4): 537-40 (Apr. 1982).

7. Sada, E., and Y. Takada, "Chemical Reactions Accompanying Absorption of NO into Aqueous Mixed Solutions of Fe(II)*EDTA and Na₂SO₃," *Ind. Eng. Chem. Fundam.* 23(1):60-64 (Jan. 1984).

8. Zang, V., and R.V. Eldik, "Kinetics and Mechanism of the Autoxidation of Iron(II) Induced through Chelation by EDTA and Related Ligands," *Inorg. Chem.* 29(9):1705-11 (Sept. 1990).

List of Figure Captions

- 1 Mass Balance for NO in the Gas Phase
- 2 Mass Transfer in a Gas Bubble
- 3 Correlation of Observed Nitric Oxide Transfer Units with Observed Ferrous Concentration
- 4 Schematic of Sulfite/Bisulfite Ions' Role in Simultaneous NO_x/SO₂ Removal
- 5 Percent of Total Iron as Ferrous for Different Iron:Sulfite Ratios with Sodium Ascorbate

FIGURES

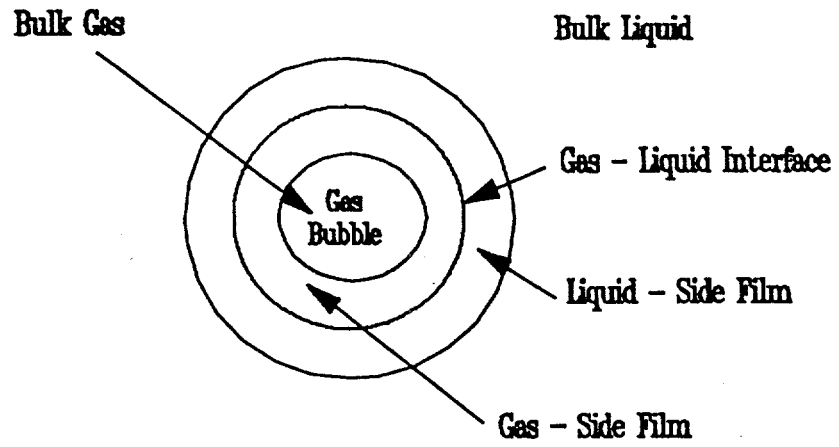


Figure 1 Mass Balance for NO in the Gas Phase

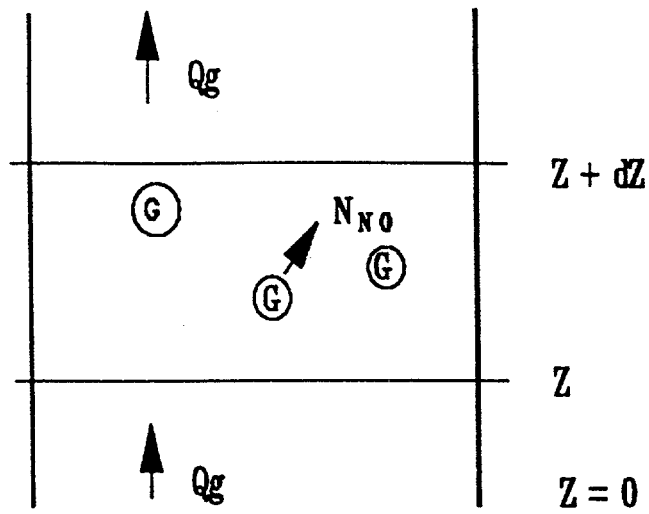


Figure 2 Mass Transfer in a Gas Bubble

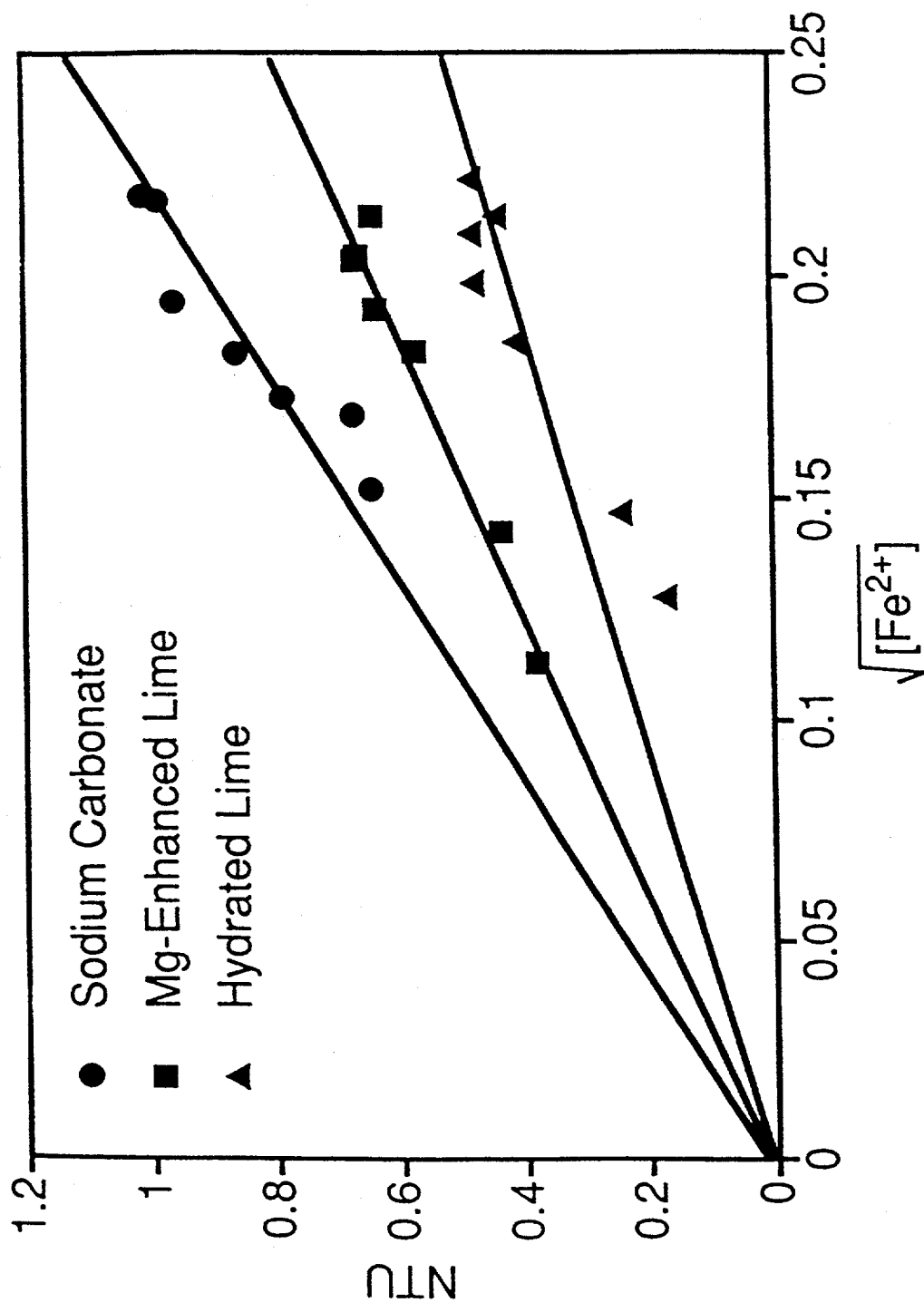


Figure 3 Correlation of Observed Nitric Oxide Transfer Units with Observed Ferrous Concentration

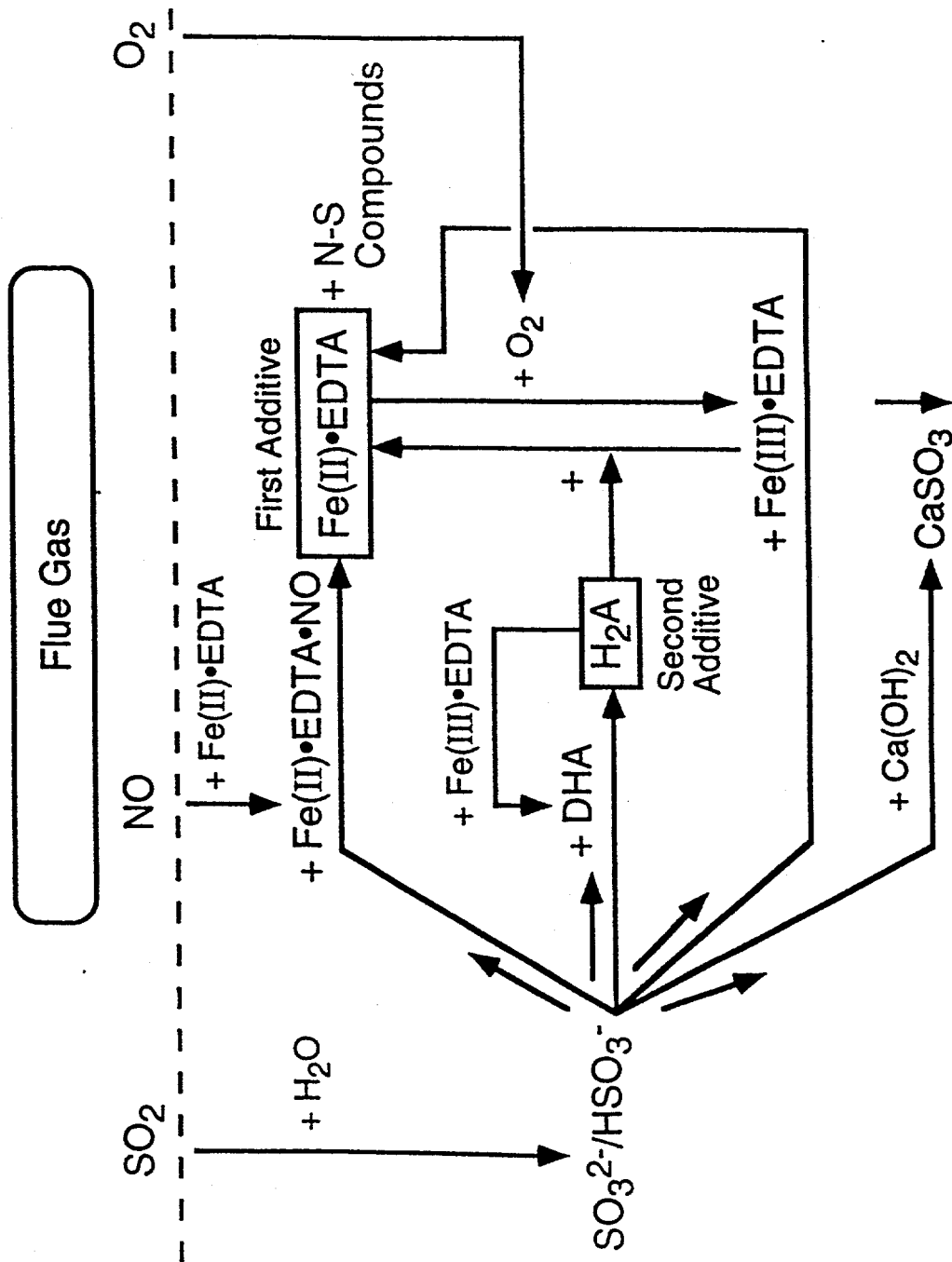


Figure 4 Schematic of Sulfite/Bisulfite Ions' Role in Simultaneous NO_x/SO₂ Removal

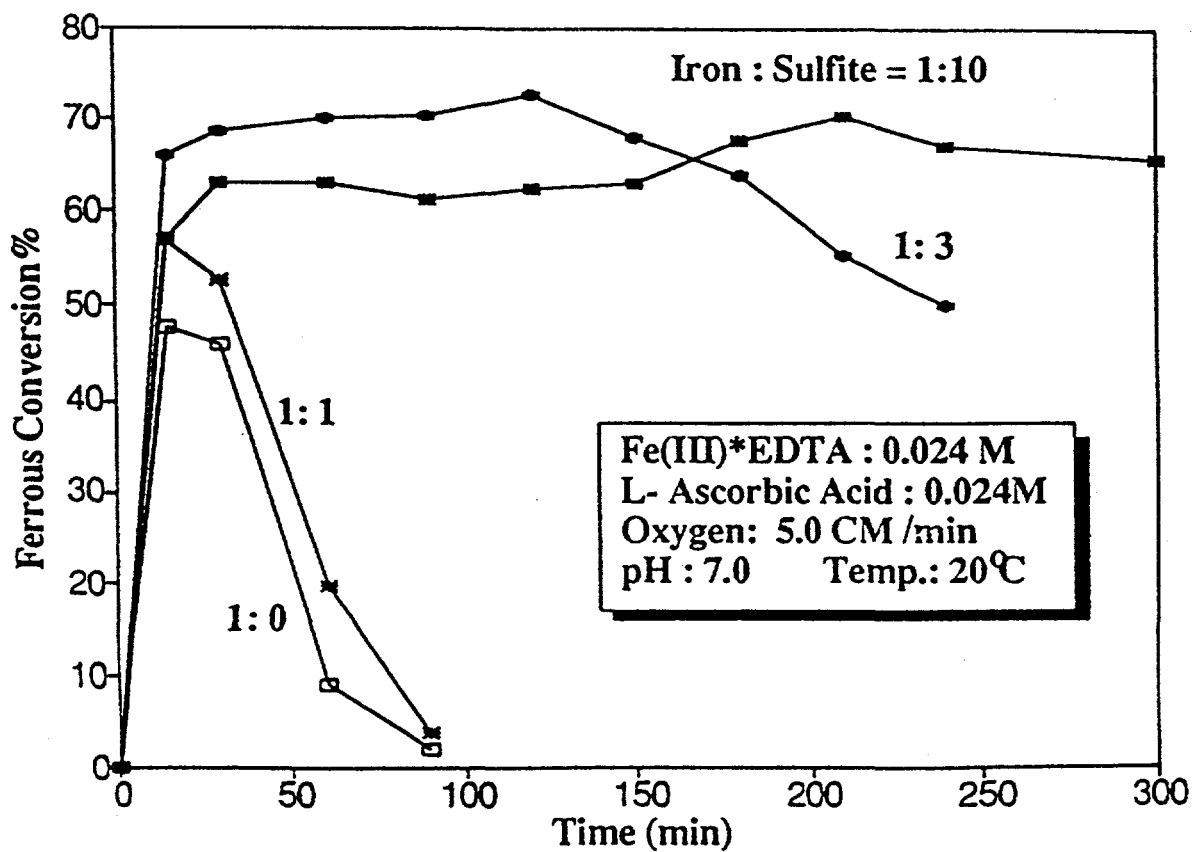


Figure 5 Percent of Total Iron as Ferrous for Different Iron:Sulfite Ratios with Sodium Ascorbate